RSC Advances

PAPER

View Article Online
View Journal | View Issue

Cite this: *RSC Adv.*, 2025, **15**, 46727

Cr(III)-salophen catalysts: efficient single-component and binary systems for sustainable CO_2/cyclohexene oxide copolymerization

Daniela Fonseca-López, *[a] David Ezenarro-Salcedo, †[a] Javier Martínez, [b] René S. Rojas *[c] and John J. Hurtado *[a]

Received 7th November 2025
Accepted 17th November 2025

DOI: 10.1039/d5ra08569a

rsc.li/rsc-advances

The rise in carbon dioxide (CO_2) emissions and the accumulation of human-made CO_2 in the atmosphere are recognized as the primary causes of the greenhouse effect. Therefore, one strategy to address this issue is capturing and utilizing CO_2 as a raw material for producing high-value chemical compounds. The most promising reactions involve the catalytic conversion of CO_2 with epoxides to produce polycarbonates (PC). For this purpose, Co(III) and Cr(III) complexes (**Cat1–Cat9**) with salophen-type ligands were synthesized and tested as catalysts for the copolymerization of cyclohexene oxide (CHO) with CO_2 to create poly(cyclohexene)carbonate (PCHC). Their catalytic activity was initially assessed in single-component systems at 100 °C and 8 bar of CO_2 for 24 hours, where **Cat5** demonstrated the highest selectivity. Subsequent optimization studies explored the effect of solvents, CO_2 pressure, and co-ligand variation. The best performance was obtained with the **Cat5**:DMAP binary system, producing a semi-crystalline PCHC copolymer with a high degree of isotacticity.

Introduction

Most of the world's energy is generated by burning fossil fuels such as coal, oil, and natural gas.[1] However, these will likely remain the predominant energy source for the next 30 years.[2–4] However, this dependence has significant environmental consequences, as it inevitably results in the emission of large amounts of CO_2, the principal greenhouse gas, into the atmosphere. These emissions have increased by more than 40% since the beginning of the Industrial Revolution, rising from a pre-industrial level of 280 ppm to 410 ppm in 2018.[5,6] According to projections by the Intergovernmental Panel on Climate Change (IPCC), the atmospheric concentration of CO_2 could reach 570 ppm in 2100. In June 2025, the monthly average CO_2 emissions reached a record high of 429.61 ppm, up from 415.2 ppm in April 2021.[7–9] To address this problem, a strategy based on the principles of the circular economy is required. In particular, carbon capture and utilization (CCU), using CO_2 as a feedstock to obtain value-added products.[10–12] CO_2 is a renewable source of carbon with multiple advantages, including its abundance, low cost, non-toxicity, and non-flammability.[12] However, it is a difficult molecule to activate, resulting in high thermodynamic stability ($\Delta G_f^0 = -394.228$ kJ mol^{-1}) and low reactivity.[13,14] Nevertheless, reacting CO_2 with high-energy substrates (hydrogen, amines, or epoxides) can overcome this low thermodynamic stability.[15–17] Among the various efforts to use CO_2 as a feedstock, the catalyzed copolymerization reaction between CO_2 and epoxides results in cyclic carbonates (CC) or in polycarbonates (PC) formation. The latter have become an attractive option at the industrial level due to their atom efficiency and their greater respect for environmental sustainability (Scheme 1).[17–19] CCs have been widely used as polar aprotic solvents,[20] electrolytes for lithium-ion batteries,[21] and in the pharmaceutical industry.[2,7,22] On the other hand, PCs have been proposed as alternatives to petroleum-derived chemicals in industries such as automotive, medical, and electronics. They are also used as starting materials for manufacturing polyurethanes.[23–25] In recent years, this research has seen

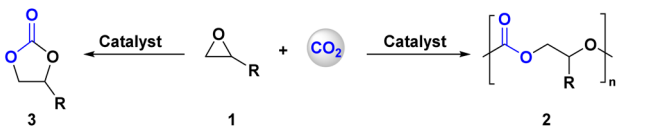

Scheme 1 Copolymerization between epoxides and CO_2 using a catalyst to obtain cyclic carbonates (**1**) or polycarbonates (**2**).

[a]*Grupo de Investigación en Química Inorgánica, Catálisis y Bioinorgánica, Departamento de Química, Facultad de Ciencias, Universidad de Los Andes, Carrera 1 No. 18A-12, Bogotá 111711, Colombia. E-mail: jj.hurtado@uniandes.edu.co; d.fonseca100@uniandes.edu.co*

[b]*Facultad de Ciencias Químicas y Farmacéuticas, Departamento de Química Orgánica y Fisicoquímica, Universidad de Chile, Santiago 8380492, Chile*

[c]*Laboratorio de Química Inorgánica, Facultad de Química y de Farmacia, Pontificia Universidad Católica de Chile, Santiago 6094411, Chile*

† Current address: David Ezenarro-Salcedo, Organometallic CO_2 Chemistry, Molecular Catalysis, Max-Planck-Institut für Kohlenforschung (MPI CEC), Stiftstraße 34–36, 45470 Mülheim an der Ruhr, Germany.

further development, with numerous studies focusing on generating catalysts that can synthesize CCs or PCs using CO_2.[5,21,26–29]

The most studied catalytic systems are coordination complexes, as they can exhibit excellent activity and selectivity for the preparation of CCs or PCs.[30,31] The well-established epoxide activation mechanism governs the synthesis of CC and applies to a wide range of catalytic systems, both metallic and non-metallic.[32–35] The most commonly reported catalytic systems use Al(III) as the metal center. However, due to the instability of these complexes in air and humidity, other metals such as Zn(II), Co(III), Cr(III), and Fe(III) become interesting.[8,32] Catalytic complexes generally contain a Lewis acid (LA), which is the metal center responsible for activating the epoxide through coordination.[33,36–38] Additionally, the presence of a nucleophile is essential for opening the epoxide ring, and it is usually part of the co-catalyst.[39,40] These catalytic systems can be classified into three groups: binary, bifunctional, and single-component.[3,32,38,41–44] Binary systems, or first-generation systems, are those in which the LA and the nucleophile exist in two separate compounds.[18] In these systems, the LA is the metal in the complex, while the nucleophile co-catalysts are usually halides from onium salts, such as tetrabutylammonium (TBA) and bis(triphenylphosphine)iminium (PPN) cations, and phenyltrimethylammonium tribromide (PTAT). Additionally, Lewis bases such as dimethylaminopyridine (DMAP), *N*-methylimidazole (NMeIm), pyridine (Py), 1,8-diazabicyclo[5.4.0]undec-7-ene (DBU), and 1,5,7-triazabicyclo[4.4.0]dec-5-ene (TBD) are widely used to carry out this process. Generally, an ideal co-catalyst consists of a bulky, non-coordinating cation paired with a nucleophilic anion.[21,45]

On the other hand, second-generation catalytic systems were developed, in which the co-catalyst is covalently bound to the main ligand, known as bifunctional systems. In these systems, both the LA and the nucleophile are contained within a single molecular entity, meaning the nucleophile is part of the functionalization of the ligand.[46,47] Generally, these systems consist of protic tetraalkylammonium halides, protic phosphonium halides, among others.[18,24] These changes have resulted in increased selectivity for PC formation over CC formation, as the ammonium arms prevent the cyclization of the anionic polymer chain through electrostatic interactions. In addition, these bifunctional catalysts enable reduced catalyst loadings while maintaining high selectivity even at elevated temperatures, thereby enhancing overall reactivity.[25,48,49] Finally, the latest generation of homogeneous catalysts, known as single-component catalysts, is characterized by the absence of a co-catalyst and the presence of a nucleophile directly attached to the metal, serving as its counterion. Several bimetallic catalysts have been synthesized in this category.[36,50] However, there are only a few reports in the literature based on monometallic catalysts of this class, the first being an Al(III) complex derived from a bis(amidinato) ligand.[33] The most widely used catalysts are highly efficient and selective homogeneous metal-based complexes. Representative examples include complexes with ligands such as porphyrins, aminophenolates, β-imidinates, amidinates, heteroscorpionates, salen, and macrocycles. These catalysts typically enable synthesis at room temperature (25–100 °C) and CO_2 pressures ranging from 1 to 100 bar.[3,20,28,33,34,36,39,42,49–52] Although various metal-based catalytic systems have been explored for this transformation, a key challenge remains: the development of catalysts that are not only highly active and selective but also easy to synthesize, air-stable, and based on metals with relatively low toxicity. In this context, Cr(III) and Co(III) complexes have become highly effective and selective catalysts for forming CC and PCs, demonstrating excellent performance under mild conditions. These catalysts not only provide promising activity and selectivity but also offer improved air and moisture stability compared to traditional Al(III) systems. This enhanced robustness facilitates handling and storage, making them highly attractive candidates for CO_2-based polymerization. In this context, this work will focus on evaluating the catalytic performance of Cr(III) and Co(III) complexes derived from salophen ligands in the production of poly(cyclohexene carbonate) (PCHC) *via* the copolymerization of cyclohexene oxide (CHO) and CO_2. Through this study, we aim to contribute to the development of efficient catalysts for sustainable polymer synthesis.

Results and discussion

Salophen-type Co(III) and Cr(III) complexes **Cat1–Cat9** (Scheme 2) were prepared in excellent yields, as previously reported,[53,54] and tested as catalysts for the copolymerization reaction between CHO and CO_2. It is known that the reaction for producing PCHC yields a mixture of cyclohexene carbonate (CHC-*trans*) and polyether (PE), the latter formed from consecutive epoxide insertions. These by-products arise from competing propagation and backbiting reactions, which reduce the selectivity toward PCHC.[55]

Firstly, the single-component catalysts **Cat1–Cat6** were tested for the obtention of PCHC using a 0.5 mol% catalyst loading for 24 h at room temperature and 1 bar of CO_2 pressure without a cocatalyst. Under these conditions, no conversion to PCHC was observed. Therefore, we decided to increase the CO_2 pressure and temperature to 8 bar and 100 °C, respectively, while maintaining all other conditions constant. Co(III) complexes **Cat1**, **Cat2**, and **Cat3** achieved conversions of 37%, 31% and 49%, respectively; however, PE was the only product obtained. Subsequently, increasing the catalyst loading to 1 mol% (8 bar, 100 °C, 24 h) improved conversions to 60%, 57% and 41%, respectively, although PE remained the only product.

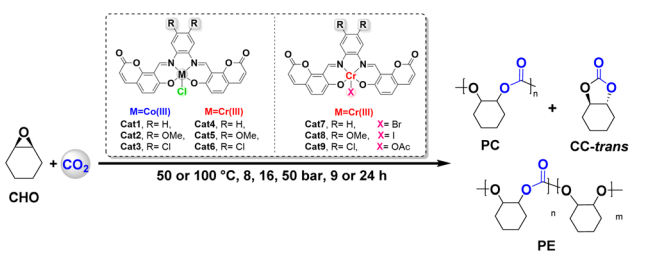

Scheme 2 Synthesis of PCHC catalyzed by Co(III) and Cr(III) **Cat1–Cat9** catalyst complexes.

Table 1 Synthesis of PCHC catalyzed by complexes **Cat1–Cat9**[a]

Entry	Cat. (mol%)	Time (h)	% Conv.[b]	% CHC[b]	% Copolymer (% carbonate linkage)[b]	TON[c]	TOF[d] (h^{-1})
1	**Cat1 (0.5)**	24	37	0	37 (0)	74	3.07
2	**Cat2 (0.5)**	24	31	0	31 (0)	62	2.58
3	**Cat3 (0.5)**	24	49	0	49 (0)	98	4.07
4	**Cat4 (0.5)**	24	64	3	97 (47)	128	5.34
5	**Cat5 (0.5)**	24	68	2	98 (54)	136	5.65
6	**Cat6 (0.5)**	24	41	0	100 (16)	82	3.42
7	**Cat1 (1)**	24	60	0	60 (0)	60	2.49
8	**Cat2 (1)**	24	57	0	57 (0)	57	2.37
9	**Cat3 (1)**	24	41	0	41 (0)	41	1.70
10	**Cat4 (1)**	24	69	2	98 (48)	69	2.88
11	**Cat5 (1)**	24	79	2	98 (61)	79	3.29
12	**Cat6 (1)**	24	70	1	99 (8)	70	2.92
13	**Cat5 (0.5)**	9	42	3	97 (35)	84	9.31
14	**Cat7 (0.5)**	9	33	15	85 (5)	66	7.31
15	**Cat8 (0.5)**	9	27	0	27 (0)	54	5.98
16	**Cat9 (0.5)**	9	30	0	30 (0)	60	6.65
17	**Cat5 (1)**	9	50	3	97 (45)	50	5.54

[a] Reactions were carried out at 100 °C and 8 bar CO_2 pressure for 24 h. [b] Conversion, % of CHC-*trans*, % of PCHC, and % of carbonate linkages determined by ^{1}H NMR spectroscopy of the crude reaction mixture. [c] TON = moles of product/moles of catalyst. [d] TOF = TON/time (h); calculated from total epoxide conversion.

These results suggest that, following nucleophilic opening of the epoxide, consecutive epoxide insertion was favored over CO_2 insertion. This behavior can be attributed to the Lewis acidity of Co(III), which stabilizes the alkoxide intermediate and reduces its nucleophilicity, thereby slowing down the CO2 insertion step and resulting in remarkable selectivity toward PE formation.[51,56]

The Cr(III) complexes **Cat4**, **Cat5**, and **Cat6** displayed moderate to high activity at 0.5 mol% catalyst loading, where **Cat5** exhibited the highest selectivity toward PCHC (Table 1). When the catalyst loading was increased to 1 mol%, **Cat4–Cat6** presented higher conversions, and **Cat5** again exhibited the highest selectivity toward PCHC. This is probably due to the presence of methoxy groups on the aromatic ring enhances CO_2 insertion and copolymerization by increasing the lability of the Cr(III)-alkoxy bond. On the other hand, **Cat4** showed moderate catalytic activity due to the absence of electron donation. At the same time, **Cat6**, with electron-withdrawing groups, exhibited lower activity because the stronger Cr(III)-alkoxide interaction hinders CO_2 insertion and PCHC formation.[57,58] To investigate the effect of the coligand, Cr(III) catalysts **Cat7** (Br^-), **Cat8** (I^-), and **Cat9** (OAc^-) (Scheme 2) were designed as structural modifications of **Cat5**. The reaction time was then shortened to 9 hours while keeping the same conditions. Results showed that **Cat5** remained the most efficient catalyst under these conditions, while **Cat7–Cat9** exhibited significantly lower activity and were inactive in producing PCHC. Moreover, increasing **Cat5** loading at short reaction time did not substantially enhance PCHC selectivity. These results indicate that the difference in selectivity toward PCHC between using 0.5 mol% and 1 mol% is not significant because increasing the metal content in the system does not necessarily improve epoxide conversion activation.[59]

To enhance selectivity toward PCHC, a co-catalyst was added, as previous studies have confirmed that introducing a nucleophile source as a co-catalyst improves copolymerization selectivity (Table S1).[60–62] It is important to note that before this step, the co-catalysts were tested individually and showed no conversion to PCHC or CHC.

Using DMAP as a co-catalyst (0.5 : 0.5 mol% ratio, 8 bar CO_2, 100 °C, 24 h), **Cat1–Cat3** exhibited low selectivity toward PCHC, and were therefore excluded from further evaluation.[63–65] In contrast, catalysts **Cat4–Cat6** were tested with each of the co-catalysts (DMAP, PPNCl, TBAI, TBAC, TBAB), and **Cat5:DMAP** showed the highest selectivity toward PCHC.

These systems, **Cat5:PPNCl**, **Cat5:TBAC**, **Cat5:DMAP**, **Cat4:DMAP**, and **Cat4:TBAC**, were subsequently evaluated in THF and toluene to assess the effects of the solvent and cocatalyst, and the single-component catalysts **Cat4** and **Cat5** were also tested (Table 2). Initially, when tested in THF without a co-catalyst, **Cat4** and **Cat5** showed moderate conversion rates, but the PCHC selectivity was low in both cases, resulting in the exclusive formation of CHC-*cis*. This is attributed to the coordinating nature of THF, which promotes the early-stage formation of CHC-*cis* by competing with the growing polymer chain for coordination to the Cr(III) center. This mechanism facilitates chain release and cyclization through two SN_2 steps: epoxide ring opening followed by CO_2 insertion, and final ring closure to form the cyclic carbonate.[52,66,67] **Cat5:DMAP** showed the highest conversion among the catalytic systems in THF, due to the good solubility of DMAP in CHO.[24,68] However, PCHC was not obtained as a product in any of these assays, although CHC-*cis* and CHC-*trans* were obtained. Its formation is attributed to the depolymerization of a previously formed polymer-free anionic chain due to THF coordination. CHC-*trans* results from the cyclization of a terminal alkoxide, while CHC-*cis* forms *via* cyclization of a carbonate intermediate through two consecutive stereochemical inversions.[69,70] These findings are supported by solvent-free assays with **Cat5**, in which CHC-*cis*

Table 2 Synthesis of PCHC catalyzed by complexes **Cat4** and **Cat5** using THF[a]

Entry	Cat. (0.5 mol%)	Co-cat (0.5 mol%)	% Conv.[b]	% CHC (*cis*/*trans*)[b]	% Copolymer (% carbonate linkage)[b]	TON[c]	TOF[d] (h^{-1})
1	**Cat4**	—	54	35/0	60 (4)	108	4.49
2	**Cat4**	DMAP	30	20/52	28 (0)	60	2.49
3	**Cat4**	TBAC	16	16/27	57 (0)	32	1.33
4	**Cat5**	—	71	30/0	66 (4)	142	5.90
5	**Cat5**	DMAP	64	9/32	59 (0)	128	5.32
6	**Cat5**	PPNCl	20	5/74	21 (0)	40	1.66
7	**Cat5**	TBAC	21	4/69	27 (0)	42	1.75

[a] Reactions were carried out at 100 °C and 8 bar CO_2 pressure for 24 h. [b] Conversion, % of CHC-*trans*, % of CHC-*cis*, % of PCHC, and % of carbonate linkages determined by ^{1}H NMR spectroscopy of the crude reaction mixture. [c] TON = moles of product/moles of catalyst. [d] TOF = TON/time (h); calculated from total epoxide conversion.

was not detected and PCHC was the predominant product. When toluene was used as a solvent (Table S2), both conversion and PCHC selectivity decreased, while CHC-*trans* selectivity increased due to ring-opening polymerization followed by decarboxylation, yielding PE and CO_2.[56,71] This suggests that toluene favors depolymerization pathways, enhancing CHC-*trans* and PE formation.[72] Despite this, the highest conversion was achieved with **Cat5:DMAP**, followed by **Cat4:DMAP**. Overall, **Cat5:DMAP** showed the best performance among all binary systems tested. However, the presence of solvent did not improve the catalytic activity for PCHC production in these systems.

Based on the results obtained, it can be observed that **Cat5** exhibits the highest selectivity values towards PCHC, with and without solvent. These combinations, **Cat5:PPNCl**, **Cat5:TBAC**, and **Cat5:DMAP**, were tested at a molar ratio of 0.5 : 1 without solvent (Table 3). According to Table 3, the highest conversion and selectivity towards PCHC was achieved with the binary catalyst **Cat5:DMAP**. Therefore, the DMAP co-catalyst was chosen as the most active and was used in the other catalytic tests. Subsequently, **Cat7–Cat9** with DMAP (0.5 : 1 mol%) were also tested. Although all three catalysts showed improved selectivity towards PCHC compared to the 0.5 : 0.5 mol% ratio (Table S3), they still showed lower selectivity than the **Cat5:DMAP** system. Even without a cocatalyst, the single-component **Cat5** showed good selectivity toward PCHC (Table 1). In general, the trend of the influence of the co-ligand on catalyst activity was $Cl^- > Br^- \approx I^- > OAc^-$. This is probably because Cl^-, which acts as a co-ligand, acts as an effective nucleophile and leaving group, favoring epoxide ring opening and promoting active propagation chains over cyclization reactions toward CHC. Furthermore, to verify whether the 0.5 : 1 mol% (**Cat5:DMAP**) ratio was the most catalytically active, additional tests were performed, keeping the catalyst loading at 1 mol% and varying the co-catalyst loading to 0.5, 1, and 2 mol% (Table S3). These tests revealed that none of these three ratios exceeded the selectivity achieved with 0.5 : 1 mol% (**Cat5:DMAP**), which is currently the highest (Table 3). This suggests that the ratio between the metal (catalyst) and the anion (co-catalyst) is more critical than the actual amount of metal (catalyst) present in the reaction mixture.

The effect of increasing CO_2 pressure from 8 bar to 16 bar was examined using the single-component **Cat5** catalyst and the **Cat5:DMAP** catalytic system at 100 °C for 24 hours. Initially, with **Cat5** loadings of 0.5 mol% and 1 mol%, the variation in selectivity towards PCHC was found to be minimal (Table S4). Similarly, using **Cat5:DMAP** at a 0.5 : 1 mol% catalyst to cocatalyst ratio, it was observed that this was the most catalytically active molar ratio at both 8 and 16 bar CO_2, with 8 bar showing the highest selectivity towards PCHC (Table 3). Along with the tests mentioned above, an experiment was carried out at 100 °C, 50 bar of CO_2 with a catalyst loading of 1 mol% **Cat5**, which resulted in good conversion and selectivity towards PCHC (Table S4). However, when comparing these results with those obtained with **Cat5** (Table 1), lower CO_2 pressures favor the formation of PCHC, while higher pressures increase the selectivity of *trans*-CHC, probably due to the depolymerization of PCHC caused by high CO_2 pressure. Furthermore, the observed decrease in selectivity may be due to dilution of the catalyst/epoxide mixture[73] or precipitation caused by increased CO_2 solubility, ultimately reducing catalytic activity.[74–76] From this, it can be concluded that the optimal pressure for catalytic tests is 8 bar of CO_2, since doubling the pressure to 16 bar did not significantly change the selectivity toward PCHC. However,

Table 3 Effect of co-catalyst on the synthesis of PCHC catalyzed by **Cat5** (0.5 mol%)[a]

Entry	Co-cat (1 mol%)	% Conv.[b]	% CHC *trans*[b]	% Copolymer (% carbonate linkage)[b]	TON[c]	TOF[d] (h^{-1})
1	DMAP	95	14	86 (77)	189	7.89
2	PPNCl	86	13	87 (69)	172	7.15
3	TBAC	88	6	94 (55)	176	7.31

[a] Reactions were carried out using 0.5 mol% **Cat5** and 1 mol% co-cat at 8 bar CO_2 pressure for 24 h at 100 °C. [b] Conversion, % of CHC-*trans*, % of PCHC, and % of carbonate linkages determined by ^{1}H NMR spectroscopy of the crude reaction mixture. [c] TON = moles of product/moles of catalyst. [d] TOF = TON/time (h); calculated from total epoxide conversion.

when the pressure is raised to 50 bar of CO_2, the PCCH production rate starts to decline.

Characterization of PCHC obtained with Cat5:DMAP

The polymerization reaction performed with the binary catalyst **Cat5:DMAP** (Table 3, entry 5) reached 95% conversion, as determined by ^{1}H NMR, with 77% selectivity toward PCHC (Fig. S2). Subsequent purification effectively removed PE from the crude mixture; however, complete elimination of CHC-*trans* remained challenging, as indicated by residual signals in the ^{1}H NMR spectrum (Fig. 1). As a result, the selectivity increased from 77% to 95%, suggesting that the initially obtained material was likely a physical mixture of PCHC and PE, rather than a true copolymer containing both ether and carbonate linkages.[77–80] In the PCHC repeating unit, the methine protons were designated as $\mathbf{H_c}$ and $\mathbf{H_c}'$, while the protons corresponding to the polymer chain end were assigned as $\mathbf{H_a}$ and $\mathbf{H_b}$. The terminal hydroxyl group was identified based on literature reports, as the chemical shift of $\mathbf{H_a}$ remains consistent across all PCHC samples, regardless of the halide initiator used.[81,82] This consistency further suggests that halogen-terminated copolymers, if present, are only present in trace amounts.[80,83]

In the ^{13}C{^{1}H} NMR spectrum of PCHC, signals corresponding to the methine carbon (a/a') were identified at 76.29 ppm and to the methylene carbons at 27.18 (b/b') and 19.58 (c/c') ppm (Fig. S3). Additionally, signals indicating the stereoselectivity and thus the tacticity of PCHC were observed in the carbonyl region of the ^{13}C NMR spectrum. The assignment of these signals was based on previous reports describing PCHC synthesized from copolymerization between CHO and CO_2.[84] The stereoselectivity of a PCHC is determined by the relative stereochemistry of the carbons of the cyclohexane units into which the main chain enters. Literature consistently reports a *trans* orientation of the entry and exit bonds in these rings.[85,86]

According to convention, [m] and [r] refer to meso and racemic dyads, respectively, depending on whether the incorporated monomer units have identical or opposite configurations.[84,87] Tetrads arise from combinations of such dyads and are classified as isotactic ([m]) or syndiotactic ([r]), as illustrated in Fig. 2.[88] Isotactic sequences (RR–RR or SS–SS) yield highly ordered PCHC, while alternating RR–SS configurations form syndiotactic chains.[89,90] In the carbonyl region (152–156 ppm), two signals were detected: a low-intensity peak at 155.61 ppm (15%) assigned to syndiotactic tetrads, and a more intense signal at 155.91 ppm (85%) attributed to isotactic tetrads (Fig. 2). These results indicate a predominantly ditactic microstructure, favoring crystallization.[85,89]

The formation of PCHC was further confirmed by comparing the FT-IR spectra of CHO and PCHC (Fig. S4).[91] Two strong absorption bands were observed at 1755 and 1261 cm^{-1}, corresponding to the C=O and C–O stretching vibrations of the linear carbonate bond, respectively. Additional bands at 2931 and 2862 cm^{-1} were assigned to the asymmetric and symmetric stretching modes of the CH_2 groups.[92,93] The thermal properties of PCHC were investigated by thermogravimetric analysis (TGA) and differential scanning calorimetry (DSC). PCHC exhibited thermal behavior consistent with a semicrystalline polymer. TGA analysis showed thermal stability up to 120 °C, followed by 95% mass loss and a decomposition onset at 220 °C (Fig. S5). DSC analysis revealed a glass transition (T_g) at ~50 °C (Fig. S6), indicative of relatively high chain mobility.[89–91] A crystallization exotherm at 60.7 °C ($\Delta H_c = 2.47$ J g^{-1}) and a melting endotherm at 171.0 °C ($\Delta H_f = 4.04$ J g^{-1}) confirmed the semicrystalline nature of the polymer and its suitability for thermoplastic processing.[94,95] Overall, despite its semicrystalline character, the moderate crystallinity and relatively low T_g suggest that PCHC retains adequate chain mobility for conventional thermoplastic processing. Thus, the material should balance mechanical integrity with good processability under standard thermoplastic conditions. Finally, ESI-MS analysis of the crude product revealed two series of PCHC chains (● and ■), attributed to distinct initiation pathways involving the **Cat5:DMAP** binary system (Fig. S7). Both series showed regular *m*/*z* spacing of 142, corresponding to the carbonate–cyclohexane repeat unit.[93,96,97]

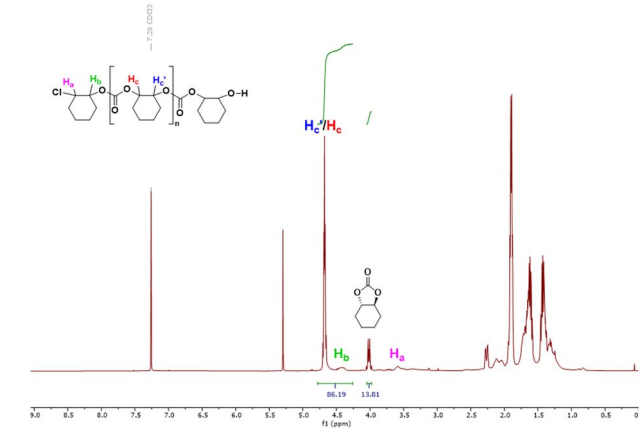

Fig. 1 ^{1}H} NMR spectrum of PCHC obtained using **Cat5:DMAP** in $CDCl_3$. Signals H_a and H_b are attributed to the terminal methine protons of the copolymer, while H_c/H_c' correspond to the methine protons within the copolymer backbone. Additionally, the signal at 4.0 ppm corresponds to 14% of the CHC-*trans*.

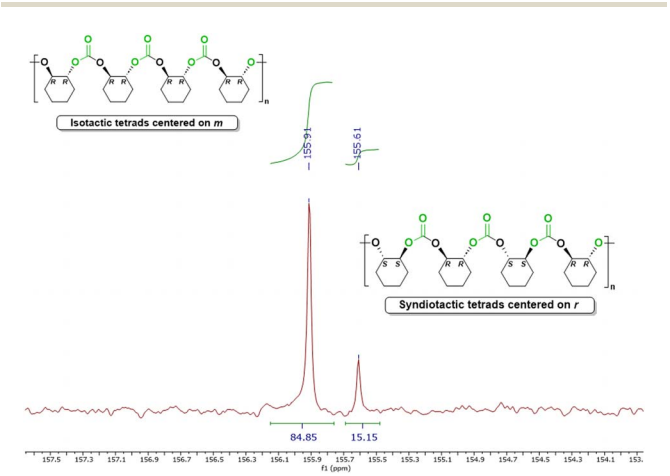

Fig. 2 Carbonyl region of the ^{13}C{^{1}H} NMR spectrum in $CDCl_3$ of PCHC obtained using **Cat5:DMAP**.

Series ● was assigned to chains with hydroxyl termini, resulting from chain transfer from chloride to water.[20,98] Series ■ contained DMAP as the initiator and a hydroxyl end group, consistent with epoxide ring-opening initiated by DMAP (Fig. S8). In both cases, hydroxyl termination is attributed to HCl-induced hydrolysis. The mass distribution confirms the alternating structure of the copolymer.

Finally, the molecular weight (M_{nexp}) and polydispersity (PDI) of the obtained PCHC catalyzed by **Cat5:DMAP** were determined by gel permeation chromatography (GPC) calibrated with PMMA standards in chloroform (Table S5 and Fig. S9). It is relevant to comment that the PDI (M_w/M_n) observed was 1.06, indicating a narrow molecular weight distribution. This low PDI is characteristic of a well-controlled polymerization process, suggesting that the catalyst system effectively mediates the ring-opening copolymerization (ROCOP) of CO_2 and CHO with minimal side reactions or chain-transfer events. The M_n value observed (18 797 Da) reflects a high molecular weight, suitable for applications where mechanical robustness and thermal stability are desired.[99,100] These results highlight the potential of **Cat5:DMAP** as a highly selective catalyst system in producing uniform PCHC chains, which is particularly relevant for tuning polymer properties in advanced material applications.

Proposed mechanism for Cat5:DMAP catalyzed CHO/CO_2 copolymerization

According to the results obtained when using the binary catalyst **Cat5:DMAP**, the possible formation of a hexacoordinated complex was proposed, commonly observed when using a pentacoordinate (salophen)Cr(III)X complex (**A**) in the presence of a co-catalyst nucleophile (Nu) (Scheme 3).[101–103] An equilibrium between a mono-DMAP species (**B**) and a hexacoordinated cationic complex (**C**) with two DMAP molecules was suggested.

In the presence of excess epoxide, these two intermediates underwent competitive binding with CHO to form species (**D**) and (**E**), activating the epoxide. CHO activation can proceed *via* two possible pathways: either through an intramolecular nucleophilic attack on the coordinated CHO (**F**), or *via* ring-opening promoted by the external co-catalyst nucleophile (**G**). In both cases (Nu = Cl^-, DMAP), the nucleophile initiates polymerization and becomes incorporated into the growing chain. Coordination of CHO to Cr(III) weakens the adjacent metal–Nu_1 bond, enabling rapid epoxide ring-opening (**H**). When DMAP binds *trans* to the propagating chain, it facilitates CO_2 insertion by weakening the metal–alkoxide bond, leading to the initial carbonate complex (**I**) (Scheme 4).[24,105] Intermediate (**I**) then undergoes CHO insertion, likely *via* nucleophilic attack by a second metal-bound nucleophile rather than by the growing polymer chain, resulting in intermediate (**J**). Subsequent CO_2 insertion yields intermediate (**K**), from which

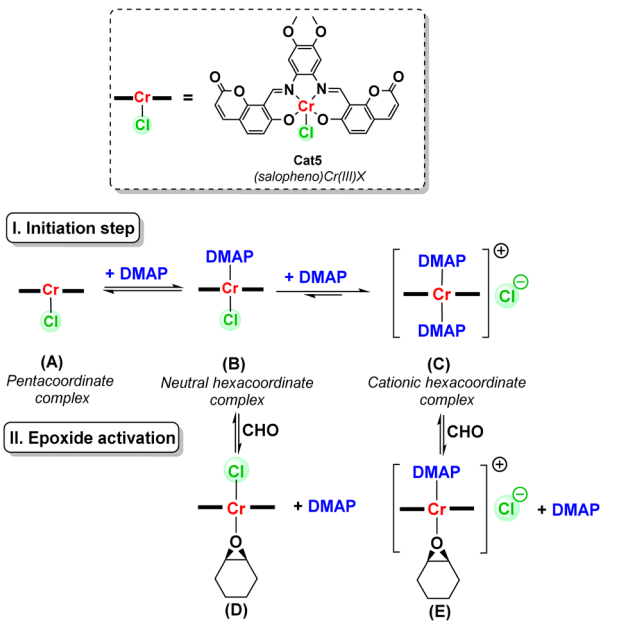

Scheme 3 Initiation stage and formation of the hexacoordinate complex.

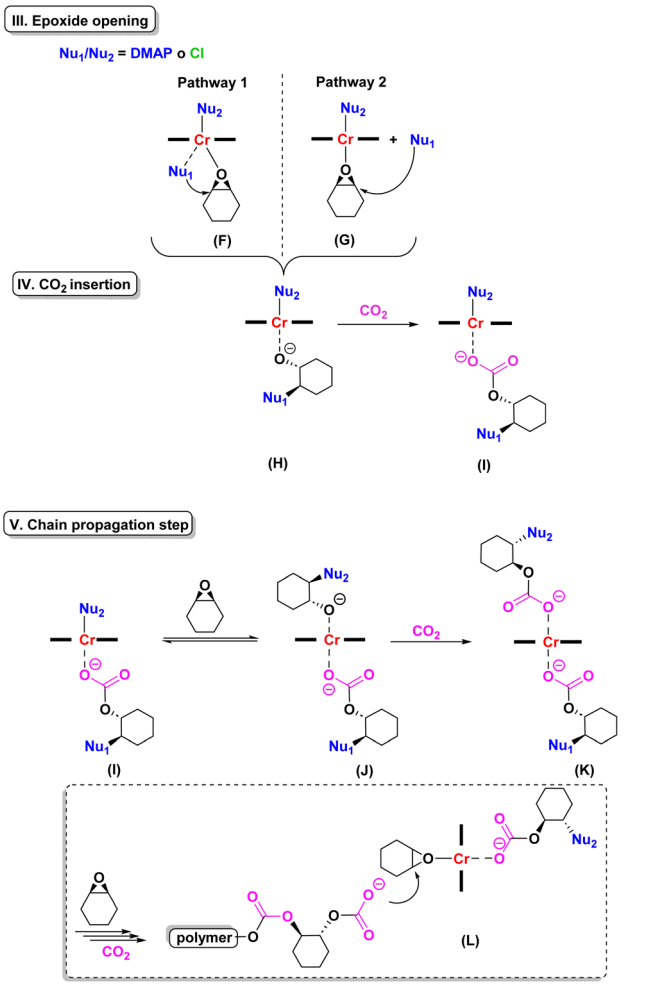

Scheme 4 Epoxide ring-opening through pathway 1 and pathway 2, followed by CO_2 insertion and chain propagation step, after consecutive CO_2 and CHO insertions.

alternating CHO and CO_2 insertions occur at the active chain ends. This enables the simultaneous growth of two polymer chains from the metal center, producing the intermediate (**L**). This alternation is due to the planar nature of the salophen ligand, a structural feature transferred to the complex (Scheme 4).[24,104] Alternatively, a complementary hypothesis might explain the higher conversion and selectivity observed with the binary **Cat5:DMAP** catalyst compared to the single-component **Cat5**. This involves an alternative initiation mechanism, in which CO_2 incorporation occurs before epoxide activation, a pathway often seen when *N*-heterocyclic amines are used as co-catalysts.[24,102] However, further mechanistic studies are needed to confirm this. It is proposed that DMAP activates CO_2 in two steps: first, they interact with CO_2 in the presence of (salophen) Cr(III)X (**Cat5**), forming a weakly stabilized carbamate zwitterionic intermediate *via* a bidentate complex (Scheme S1). This intermediate then reacts with CHO, producing a stabilized zwitterionic intermediate. This mechanism aligns with those proposed in the literature for related systems.[104]

Additionally, increasing the DMAP loading from 0.5 to 2 mol% (Table S3, entries 4–6) led to lower PCHC selectivity, suggesting that the mono-DMAP intermediate (**B**) is more catalytically active than the bis-DMAP cationic complex (**C**). While intermediate (**B**) is expected at **Cat5:DMAP** ratios of 0.5 : 0.5 (Table S1, entry 5) or 1 : 1 (Table S3, entry 5), high selectivity was not observed under these conditions. This implies that a slight excess of DMAP (0.5 : 1 ratio) (Table 3, entry 1) is necessary to favor an optimal equilibrium between intermediates (**B**) and (**C**), thereby promoting the formation of active species (**D**) and (**E**). In contrast, an excess of DMAP (1 : 2 ratio) (Table S3, entry 6) likely shifts the equilibrium toward (**C**), which reduces selectivity by displacing the growing polymer chain and favoring depolymerization *via* backbiting. Mass spectrometric (HRMS) evidence supports the coexistence of both species at the 0.5 : 1 mol% (Table 3, entry 1) **Cat5:DMAP** ratio. At lower DMAP loadings, the major species detected corresponded to intermediate (**B**), observed as a sodium adduct with the molecular formula $[C_{35}H_{28}ClCrN_4O_8Na]$ and a m/z = 742.0818, in agreement with the theoretical value of 742.0898 m/z (Fig. 3a). Upon addition of an extra equivalent of DMAP, a new peak appeared with the molecular formula $[C_{42}H_{38}CrN_6O_8]^+$ and a m/z = 806.2131, matching the theoretical value for intermediate (**C**) of 806.2156 m/z (Fig. 3b). The simultaneous presence of both signals indicates an equilibrium between these complexes, consistent with their proposed role in CHO activation. Conductivity measurements further supported the HRMS results. At a 0.5 : 0.5 **Cat5:DMAP** ratio, the solution exhibited a molar conductivity of 57.6 Ω^{-1} cm^2 mol^{-1}, consistent with the formation of a neutral species, attributed to intermediate (**B**).[105] Upon increasing the DMAP ratio to 0.5 : 1, the conductivity increased to 63 Ω^{-1} cm^2 mol^{-1}, approaching the value expected for a 1 : 1 electrolyte (65 Ω^{-1} cm^2 mol^{-1}). This shift aligns with the formation of cationic intermediate (**C**), reinforcing the coexistence of both species in solution.

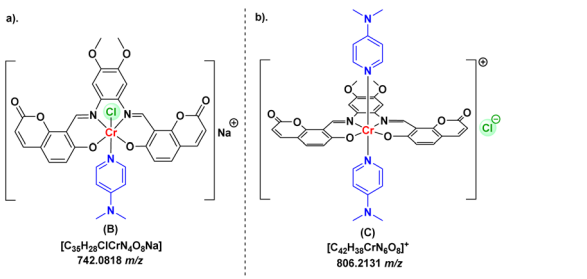

Fig. 3 (a). Intermediate [(**B**) + Na], and (b). Intermediate (**C**), identified by HRMS (ESI-MS).

Experimental

Methods and general procedures

All chemicals were purchased from commercial suppliers (Merck and Aldrich). 7-Hydroxycoumarin, trifluoroacetic acid, acetic anhydride, sodium bicarbonate, *o*-phenylenediamine, 4,5-dichloro-*o*-phenylenediamine, hexamine, catechol, methyl iodide, Pd/C 10 wt%, hydrazine monohydrate. Commercial CO_2 was obtained from Gas-Lab and used without further purification. The commercially available cyclohexene oxide (CHO) (99.8%) was purchased from Sigma-Aldrich. Fourier transform infrared (FTIR) spectra were obtained on a Shimadzu IR Tracer-100 spectrometer using a single-reflection ATR accessory. High-resolution Mass Spectrometry (HRMS) was performed using a Micromass Quattro Q-TOF LC/MS system equipped with electrospray ionization (ESI+) ionization. The NMR spectra were recorded on a Bruker AV-400 spectrometer and referenced to the residual NMR solvent signals. Molecular weight estimations of the synthesized polymers were carried out using a gel permeation chromatograph (GPC, Jasco, Japan) equipped with a refractive index detector (RI-4030, Jasco) and a divinylbenzene-based column (DVB column, Jordi Labs) enclosed in a column oven at 40 °C (CO-4060, Jasco). A 10 mg sample of the polymer was dissolved in 1.0 mL of chloroform and stirred overnight until the total dissolution of the polymer into the solvent occurred. GPC measurements of the samples were carried out with chloroform as mobile phase at 1.0 mL min^{-1}. Molecular weight calculations (M_w, M_n, and polydispersity index) were done using ChromNAV-GPC software (Jasco), employing a molecular weight calibration curve prepared using different narrow polymethylmethacrylate (PMMA) standards (ReadyCal kit, Polymer Standard Service GmbH).

General procedure for catalyst screening

The catalyst complexes **Cat1–Cat9** were synthesized previously following previous reports in our research group.[53,54] These catalysts are stable in air and humidity, which allows for easier handling when performing catalytic tests. CHO (0.107 g, 1.09 mmol), catalysts **Cat1–Cat9** 5.45 × 10^{-3} mmol (0.5 mol%) and 0.0109 mmol (1 mol%), and co-catalyst TBAI, TBAB, TBAC, PPNCl, or DMAP (0.5 mol%/1 mol%) were placed in a steel reactor with a magnetic stirrer bar. The autoclave was sealed, pressurized to 8–50 bar with CO_2, and heated to the desired temperature, 50 °C/100 °C. The reaction mixture was heated at

50–100 °C for 24 h. Finally, the reaction was stopped, and the reactor was carefully cooled in a liquid nitrogen bath. The conversion of the CHO to PCHC was determined by analyzing the crude reaction product using ^{1}H NMR spectroscopy. PCHC is a known compound, and the spectroscopic data of samples prepared using catalysts **Cat1–Cat9** were consistent with those reported in the literature.

Purification of PCHC

The crude product was dissolved in 20 mL of MeOH and extracted with 5 mL portions of hexane. The combined hexane layers were collected in a round-bottom flask and evaporated under reduced pressure. The residue was treated with 5 mL of 1 M HCl, affording a white precipitate corresponding to PCCH. The PCHC obtained was analyzed by various techniques, ^{1}H and ^{13}C{^{1}H} NMR, FTIR, TGA/DSC, ESI-MS, and GPC.

Conclusions

Nine air-stable Co(III) and Cr(III) complexes (**Cat1–Cat9**) with coumarin-derived salophen-type ligands were evaluated as single-component and binary catalysts in the presence of co-catalysts such as TBAB, TBAC, TBAI, PPNCl, and DMAP in the copolymerization of CO_2 and CHO to produce PCHC. Among them, **Cat5** stood out and was the most selective for obtaining PCHC with a selectivity of 54% (0.5 mol%) and 61% (1 mol%) at 100 °C and 8 bar of CO_2 for 24 hours. Similarly, under the same conditions, **Cat5:DMAP** in a 0.5 : 1 mol% (cat: co-cat) ratio was the binary system that allowed up to 77% selectivity towards PCHC. However, the use of solvents such as THF and toluene in the reaction was ruled out because no increase in selectivity towards PCHC was observed, but in some cases, the selectivity towards CHC-*trans* and CHC-*cis* increased. Likewise, **Cat7** (Br^-), **Cat8** (I^-), and **Cat9** (OAc^-) were tested as a structural modification of **Cat5**, where the trend of the influence of the co-ligand on the activity of the catalyst was $Cl^- > Br^- \approx I^- > OAc^-$. By varying the pressure (8/16/50 bar CO_2), it was concluded that the best results were obtained at a pressure of 8 bar CO_2, since using higher CO_2 pressures caused the depolymerization of PCHC. Finally, the PCHC obtained with this **Cat5:DMAP** binary catalyst can be described as ditactic, with a repeating unit of 142 *m*/*z*, composed mainly of syndiotactic (15%) and isotactic (85%) tetrads. Furthermore, thanks to its high percentage of isotacticity, it is classified as a semi-crystalline copolymer, which was confirmed by DSC analysis, showing a T_c of 60.7 °C and a T_g of ~50 °C. This synthesis of PCHC from epoxides and CO_2 is a good start towards the development of a more environmentally friendly route, offering materials with excellent properties for various applications.

Author contributions

The manuscript was written through the contributions of all authors. All authors have approved the final version of the manuscript.

Conflicts of interest

There are no conflicts to declare.

Data availability

The data underlying this article are available in the supplementary information (SI). Supplementary information: the optimization tables and the characterization of poly(cyclohexene carbonate) (PCHC). See DOI: https://doi.org/10.1039/d5ra08569a.

Acknowledgements

J. J. H., D. F. L., and D. E. S. acknowledge the Facultad de Ciencias and Chemistry Department at the Universidad de los Andes for providing funding (Project INV-2025-213-3347). J. M. is grateful for FONDECYT Iniciación Fellowship 11230124. R. R. acknowledges project FONDECYT 1230537.

Notes and references

1 R. W. Bentley, *Energy Policy*, 2002, **30**, 189–205.
2 M. Usman and A. Rehman, *RSC Adv.*, 2023, **13**, 22717–22743.
3 B. Grignard, S. Gennen, C. Jérôme, A. W. Kleij and C. Detrembleur, *Chem. Soc. Rev.*, 2019, **48**, 4466–4514.
4 R. G. Newell and D. Raimi, *Global Energy Outlook Comparison Methods: 2020 Update*, Resources for the Future Report, 2020.
5 M. Cokoja, C. Bruckmeier, B. Rieger, W. A. Herrmann and F. E. Kühn, *Angew. Chem., Int. Ed.*, 2011, **50**, 8510–8537.
6 V. Butera, L. D'Anna, S. Rubino, R. Bonsignore, A. Spinello, A. Terenzi and G. Barone, *J. Phys. Chem. A*, 2023, **127**, 9283–9290.
7 T. Yan, H. Liu, Z. X. Zeng and W. G. Pan, *J. CO2 Util.*, 2023, **68**, 102355.
8 C. Martín, G. Fiorani and A. W. Kleij, *ACS Catal.*, 2015, **5**, 1353–1370.
9 Trends in CO2 - NOAA Global Monitoring Laboratory, https://gml.noaa.gov/ccgg/trends/mlo.html, accessed July 29, 2025.
10 *The Circular Economy: Meeting Sustainable Development Goals, Issues in Environmental Science and Technology*, S. K. Ghosh and G. Eduljee, Royal Society of Chemistry, Cambridge, 2023, vol. 51.
11 A. Alhafez, E. Aytar and A. Kilic, *J. CO2 Util.*, 2022, **63**, 102129.
12 M. Aresta and A. Dibenedetto, *Dalton Trans.*, 2007, 2975–2992.
13 M. North, R. Pasquale and C. Young, *Green Chem.*, 2010, **12**, 1514–1539.
14 M. Aresta, A. Dibenedetto and A. Angelini, *Encycl. Inorg. Bioinorg. Chem.*, 2014, 1–18.
15 Q. Liu, L. Wu and R. Jackstell, *Nat. Commun.*, 2015, **6**, 5933.
16 E. Lopes and A. Ribeiro, *Catalysts*, 2020, **10**(5), 479.
17 C. Calabrese, F. Giacalone and C. Aprile, *Catalysts*, 2019, **9**, 325.

18 G. A. Bhat and D. J. Darensbourg, *Coord. Chem. Rev.*, 2023, **492**, 215277.
19 F. M. Al-Qaisi, A. K. Qaroush, K. I. Assaf, A. F. Eftaiha, I. K. Okashah, A. H. Smadi, F. Alsoubani, A. S. Barham and T. Repo, *Inorg. Chim. Acta*, 2023, **557**, 121716.
20 F. de la Cruz-Martínez, M. Martínez de Sarasa Buchaca, J. Martínez, J. Tejeda, J. Fernández-Baeza, C. Alonso-Moreno, A. M. Rodríguez, J. A. Castro-Osma and A. Lara-Sánchez, *Inorg. Chem.*, 2020, **59**, 8412–8423.
21 J. N. Appaturi, R. J. Ramalingam, M. K. Gnanamani, G. Periyasami, P. Arunachalam, R. Adnan, F. Adam, M. D. Wasmiah and H. A. Al-Lohedan, *Catalysts*, 2020, **11**, 4.
22 X. Wu, C. Chen, Z. Guo, M. North and A. C. Whitwood, *ACS Catal.*, 2019, **9**, 1895–1906.
23 Y. Liu, H. Zhou, J.-Z. Guo, W.-M. Ren and X.-B. Lu, *Angew. Chem., Int. Ed.*, 2017, **56**, 4862–4866.
24 D. J. Darensbourg, *Chem. Rev.*, 2007, **107**, 2388–2410.
25 M. Taherimehr and P. P. Pescarmona, *J. Appl. Polym. Sci.*, 2014, **131**(21), 41141.
26 J. W. Comerford, I. D. V. Ingram, M. North and X. Wu, *Green Chem.*, 2015, **17**, 1966–1987.
27 A. Deacy and J. Moreby, *J. Am. Chem. Soc.*, 2020, **142**(16), 7254–7261.
28 F. Della Monica and C. Capacchione, *J. Org. Chem.*, 2022, **11**(7), e202200300.
29 V. Adimule and B. Yallur, *J. Pharm. Invest.*, 2021, **51**, 347–359.
30 X.-F. Liu, Q.-W. Song, S. Zhang and L.-N. He, *Catal. Today*, 2016, **263**, 69–74.
31 Y. A. Alassmy, Z. Asgar Pour and P. P. Pescarmona, *ACS Sustain. Chem. Eng.*, 2020, **8**, 7993–8003.
32 Q. Song, R. Ma and P. Liu, *Green Chem.*, 2023, **25**, 6538–6553.
33 S. Saltarini, N. Villegas-Escobar and J. Martínez, *Inorg. Chem.*, 2021, **60**(2), 1172–1182.
34 Y. Rios Yepes, C. Quintero, D. Osorio Meléndez, C. G. Daniliuc, J. Martínez and R. S. Rojas, *Organometallics*, 2019, **38**, 469–478.
35 D. J. Darensbourg, *Chem. Educ.*, 2017, **94**(6), 732–737.
36 A. C. Deacy, E. Moreby, A. Phanopoulos and C. K. Williams, *J. Am. Chem. Soc.*, 2020, **142**, 19150–19160.
37 O. Chukanova and G. Belov, *Kinet. Catal.*, 2017, **58**(4), 397–401.
38 K. A. Andrea and F. M. Kerton, *Polym. J.*, 2021, **53**, 29–46.
39 G. Coates and D. Moore, *Angew. Chem., Int. Ed.*, 2004, **43**(48), 6618–6639.
40 C. Cohen and J. M. Torkelson, *J. Am. Chem. Soc.*, 2005, **127**(39), 13473–13483.
41 J. Hu, J. Ma, Q. Zhu, Q. Qian, H. Han, Q. Mei and B. Han, *Green Chem.*, 2016, **18**, 382–385.
42 Y. Rios Yepes, Á. Mesías-Salazar, A. Becerra, C. G. Daniliuc, A. Ramos, R. Fernández-Galán, A. Rodríguez-Diéguez, A. Antiñolo, F. Carrillo-Hermosilla and R. S. Rojas, *Organometallics*, 2021, **40**, 2859–2869.
43 M. Adolph, T. A. Zevaco, C. Altesleben, O. Walter and E. Dinjus, *Dalton Trans.*, 2014, **43**, 3285–3296.
44 M. Alvaro, C. Baleizao, D. Das, E. Carbonell and H. García, *J. Catal.*, 2004, **228**, 254–258.
45 R. Cauwenbergh, V. Goyal, R. Maiti, K. Natte and S. Das, *Chem. Soc. Rev.*, 2022, **51**, 9371–9423.
46 Z. Duan, X. Wang, Q. Gao, L. Zhang, B. Liu and I. Kim, *J. Polym. Sci., Part A:Polym. Chem.*, 2014, **52**, 789–795.
47 T. Ema, Y. Miyazaki, S. Koyama, Y. Yano and T. Sakai, *Chem. Commun.*, 2012, **48**, 4489–4491.
48 H. Wang, F. Xu, Z. Zhang, M. Feng, M. Jiang and S. Zhang, *RSC Sustainability*, 2023, **1**, 2162–2179.
49 S. Paul, Y. Zhu and C. Romain, *Chem. Commun.*, 2015, **51**, 6459–6479.
50 W. Lindeboom, D. A. X. Fraser, C. B. Durr and C. K. Williams, *Chem. – Eur. J.*, 2021, **27**, 12224–12231.
51 G. Luinstra, *Chem. – Eur. J.*, 2005, **11**(21), 6214–6222.
52 A. Buchard, M. R. Kember, K. G. Sandeman and C. K. Williams, *Chem. Commun.*, 2010, **47**, 212–214.
53 D. Fonseca-López, D. Ezenarro-Salcedo, F. M. Nachtigall, L. S. Santos, M. A. Macías, R. S. Rojas and J. J. Hurtado, *Inorg. Chem.*, 2024, **63**, 9066–9077.
54 D. Fonseca-López, D. Ezenarro-Salcedo, J. Zapata-Rivera, R. S. Rojas and J. J. Hurtado, *ACS Omega*, 2024, **9**, 19385–19394.
55 J. Martínez, J. A. Castro-Osma, A. Lara-Sánchez, A. Otero, J. Fernández-Baeza, J. Tejeda, L. F. Sánchez-Barba and A. Rodríguez-Diéguez, *Polym. Chem.*, 2016, **7**, 6475–6484.
56 J.-C. Lee and M. H. Litt, *Macromolecules*, 2000, **33**, 1618–1627.
57 J. A. Castro-Osma, K. J. Lamb and M. North, *ACS Catal.*, 2016, **6**, 5012–5025.
58 Z. Hošťálek, R. Mundil, I. Císařová, O. Trhlíková, E. Grau, F. Peruch, H. Cramail and J. Merna, *Polymer*, 2015, **63**, 52–61.
59 K. Hansen and J. Leighton, *J. Am. Chem. Soc.*, 1996, **118**(46), 10924–10925.
60 J. M. Longo, M. J. Sanford and G. W. Coates, *Chem. Rev.*, 2016, **116**, 15167–15197.
61 I. Grimaldi, F. Santulli, M. Lamberti and M. Mazzeo, *Int. J. Mol. Sci.*, 2023, **24**, 7642.
62 M. Martínez de Sarasa Buchaca, F. de la Cruz-Martínez, J. Martínez, C. Alonso-Moreno, J. Fernández-Baeza, J. Tejeda, E. Niza, J. A. Castro-Osma, A. Otero and A. Lara-Sánchez, *ACS Omega*, 2018, **3**, 17581–17589.
63 S. Chakravorty and B. K. Das, *Polyhedron*, 2010, **29**, 2006–2013.
64 M. Hatazawa, R. Takahashi, J. Deng, H. Houjou and K. Nozaki, *Macromolecules*, 2017, **50**, 7895–7900.
65 R. Eberhardt, *Macromol. Rapid Commun.*, 2003, **24**(2), 109–112.
66 F. Fiorentini and W. Diment, *Nat. Commun.*, 2023, **14**, 4783.
67 D. J. Darensbourg, M. J. Adams and J. C. Yarbrough, *Inorg. Chem.*, 2001, **40**, 6543–6544.
68 R. L. Paddock and S. B. Nguyen, *J. Am. Chem. Soc.*, 2001, **123**, 11498–11499.
69 F. D. Monica and A. W. Kleij, *Catal. Sci. Technol.*, 2020, **10**, 3483–3501.
70 J. H. Clements, *Ind. Eng. Chem. Res.*, 2003, **42**, 663–674.

71 D. J. Darensbourg and S.-H. Wei, *Macromolecules*, 2012, **45**, 5916–5922.
72 D. J. Darensbourg, R. M. Mackiewicz and D. R. Billodeaux, *Organometallics*, 2005, **24**, 144–148.
73 M. Super and E. J. Beckman, *Macromol. Symp.*, 1998, **127**, 89–108.
74 F. G. Denardin, S. A. B. Vieira de Melo, R. Mammucari and N. R. Foster, *Chem. Eng. Trans.*, 2013, **32**, 529–534.
75 D. J. Darensbourg, R. M. Mackiewicz, A. L. Phelps and D. R. Billodeaux, *Acc. Chem. Res.*, 2004, **37**, 836–844.
76 C. T. Cohen, C. M. Thomas, K. L. Peretti, E. B. Lobkovsky and G. W. Coates, *Dalton Trans.*, 2006, 237–249.
77 H. Sugimoto, H. Ohtsuka and S. Inoue, *J. Polym. Sci., Part A:Polym. Chem.*, 2005, **43**, 4172–4186.
78 D. J. Darensbourg, M. W. Holtcamp, G. E. Struck, M. S. Zimmer, S. A. Niezgoda, P. Rainey, J. B. Robertson, J. D. Draper and J. H. Reibenspies, *J. Am. Chem. Soc.*, 1999, **121**, 107–116.
79 K. Nozaki, K. Nakano and T. Hiyama, *J. Am. Chem. Soc.*, 1999, **121**, 11008–11009.
80 Y. Guan and X. Rui, *Chem. Rev.*, 2024, **124**(21), 12305–12380.
81 R. A. Collins, A. F. Russell and P. Mountford, *Appl. Petrochem. Res.*, 2015, **5**, 153–171.
82 K. Nakano, T. Kamada and K. Nozaki, *Angew. Chem., Int. Ed.*, 2006, **45**, 7274–7277.
83 W. Guerin, A. K. Diallo, E. Kirilov, M. Helou, M. Slawinski, J.-M. Brusson, J.-F. Carpentier and S. M. Guillaume, *Macromolecules*, 2014, **47**, 4230–4235.
84 K. Nozaki, K. Nakano and T. Hiyama, *Macromolecules*, 2001, **34**(18), 6325–6332.
85 A. K. Jassal, S. Sharma, G. Hundal and M. S. Hundal, *Cryst. Growth Des.*, 2015, **15**, 79–93.
86 W. Kuran and T. Listoś, *Macromol. Chem. Phys.*, 1994, **195**, 977–984.
87 D. J. Darensbourg and M. W. Holtcamp, *Macromolecules*, 1995, **28**(22), 7577–7579.
88 A. Yahiaoui, M. Belbachir, J. C. Soutif and L. Fontaine, *Mater. Lett.*, 2005, **59**, 759–767.
89 M. Taherimehr, S. M. Al-Amsyar, C. J. Whiteoak, A. W. Kleij and P. P. Pescarmona, *Green Chem.*, 2013, **15**, 3083–3090.
90 R. Chiarcos, K. Sparnacci, D. Antonioli, C. Ivaldi, V. Gianotti, R. Po, P. Biagini, S. Losio and M. Laus, *Eur. Polym. J.*, 2024, **214**, 113148.
91 R. Chiarcos, K. Sparnacci, D. Antonioli, S. C. Carroccio, G. Curcuruto, R. Po, P. Biagini, S. Losio and M. Laus, *Macromol. Chem. Phys.*, 2025, **226**, 2400383.
92 G.-P. Wu, W.-M. Ren and Y. Luo, *J. Am. Chem. Soc.*, 2012, **134**(12), 5682–5688.
93 G. Wu, S. Jiang, X. Lu, W. Ren and S. Yan, *Chin. J. Polym. Sci.*, 2012, **30**, 487–492.
94 R. K. Dean, L. N. Dawe and C. M. Kozak, *Inorg. Chem.*, 2012, **51**, 9095–9103.
95 K. Nakano, M. Nakamura and K. Nozaki, *Macromolecules*, 2009, **42**, 6972–6980.
96 J. Grondin and C. Aupetit, *C*, 2019, **5**, 39.
97 G. Rosetto, F. Vidal, T. M. McGuire, R. W. F. Kerr and C. K. Williams, *J. Am. Chem. Soc.*, 2024, **146**, 8381–8393.
98 G.-W. Yang, Y. Wang, H. Qi, Y.-Y. Zhang, X.-F. Zhu, C. Lu, L. Yang and G.-P. Wu, *Angew. Chem., Int. Ed.*, 2022, **61**, e202210243.
99 M. R. Kember, A. J. P. White and C. K. Williams, *Macromolecules*, 2010, **43**, 2291–2298.
100 J. Liu, W.-M. Ren, Y. Liu and X.-B. Lu, *Macromolecules*, 2013, **46**, 1343–1349.
101 B. Liu, X. Zhao, H. Guo, Y. Gao, M. Yang and X. Wang, *Polymer*, 2009, **50**, 5071–5075.
102 D. J. Darensbourg and R. M. Mackiewicz, *J. Am. Chem. Soc.*, 2005, **127**, 14026–14038.
103 D.-Y. Rao, B. Li, R. Zhang, H. Wang and X.-B. Lu, *Inorg. Chem.*, 2009, **48**, 2830–2836.
104 T. W. Yokley, H. Tupkar, N. D. Schley, N. J. DeYonker and T. P. Brewster, *Eur. J. Inorg. Chem.*, 2020, **2020**, 2958–2967.
105 I. Ali, W. A. Wani and K. Saleem, *Synth. React. Inorg., Met.-Org., Nano-Met. Chem.*, 2013, **43**, 1162–1170.